ARTICLE

BIOTECHNOLOGY and BIOENGINEERING

Impact of Initial Biofilm Growth on the Anode Impedance of Microbial Fuel Cells

Ramaraja P. Ramasamy,[1] Zhiyong Ren,[2] Matthew M. Mench,[1] John M. Regan[2]

[1]Fuel Cell Dynamics and Diagnostics Laboratory, Department of Mechanical and Nuclear Engineering, The Pennsylvania State University, University Park, Pennsylvania 16802; telephone: +1-814-863-9557; fax: +1-814-863-4848; e-mail: rur14@psu.edu

[2]Department of Civil and Environmental Engineering, The Pennsylvania State University, University Park, Pennsylvania 16802

Received 6 December 2007; revision received 21 February 2008; accepted 27 February 2008

Published online 7 March 2008 in Wiley InterScience (www.interscience.wiley.com). DOI 10.1002/bit.21878

ABSTRACT: Electrochemical impedance spectroscopy (EIS) was used to study the behavior of a microbial fuel cell (MFC) during initial biofilm growth in an acetate-fed, two-chamber MFC system with ferricyanide in the cathode. EIS experiments were performed both on the full cell (between cathode and anode) as well as on individual electrodes. The Nyquist plots of the EIS data were fitted with an equivalent electrical circuit to estimate the contributions of various intrinsic resistances to the overall internal MFC impedance. During initial development of the anode biofilm, the anode polarization resistance was found to decrease by over 70% at open circuit and by over 45% at 27 $\mu A/cm^2$, and a simultaneous increase in power density by about 120% was observed. The exchange current density for the bio-electrochemical reaction on the anode was estimated to be in the range of 40–60 nA/cm^2 for an immature biofilm after 5 days of closed circuit operation, which increased to around 182 nA/cm^2 after more than 3 weeks of operation and stable performance in an identical parallel system. The polarization resistance of the anode was 30–40 times higher than that of the ferricyanide cathode for the conditions tested, even with an established biofilm. For a two-chamber MFC system with a Nafion® 117 membrane and an inter-electrode spacing of 15 cm, the membrane and electrolyte solution dominate the ohmic resistance and contribute to over 95% of the MFC internal impedance. Detailed EIS analyses provide new insights into the dominant kinetic resistance of the anode bio-electrochemical reaction and its influence on the overall power output of the MFC system, even in the high internal resistance system used in this study. These results suggest that new strategies to address this kinetic constraint of the anode bio-electrochemical reactions are needed to complement the reduction of ohmic resistance in modern designs.

Biotechnol. Bioeng. 2008;101: 101–108.

KEYWORDS: microbial fuel cells; biofilm; internal resistance; electrochemical impedance; polarization resistance; charge transfer resistance

Introduction

In the past decade the power densities of microbial fuel cells (MFCs) have increased nearly six orders of magnitude (Logan and Regan, 2006a). The majority of this improvement has come from decreasing the system's ohmic resistance through reactor architecture modifications. For example, an early two-chamber design using a salt bridge for electrochemical connection had an overall internal resistance of 19.9 kΩ and a maximum power density of 2.2 mW/m^2 when acetate was used as the electron donor (Logan and Regan, 2006b; Min et al., 2005a). This was improved by replacing the salt bridge with a cation exchange membrane, achieving a maximum power density of 40 mW/m^2 by reducing the resistance to 1.3 kΩ (Min et al., 2005b). Integration to a single-chamber design with an air cathode and no membrane, combined with other modifications in the system architecture, reduced the resistance to 77 Ω, with a corresponding boost in power density up to 1.54 W/m^2, primarily due to the decreased solution resistance (Cheng et al., 2006; Liu and Logan, 2004; Logan and Regan, 2006b).

While modern designs have reduced ohmic resistance, little is known about other major electrochemical losses and constraints in MFC systems that affect the power output by contributing to the overall internal impedance. A recent comparison of internal resistances for three MFC designs successfully demonstrated the declining ohmic resistance between two-chamber, single chamber and membrane electrode assembly systems using the current interrupt

Correspondence to: R.P. Ramasamy

technique (Liang et al., 2007). However the current interrupt technique precludes the differentiation of the non-ohmic effects of the charge transfer resistance at the electrochemical interface (both anode and cathode), the electrochemical double layer capacitance at the electrodes, and the mass transfer resistances due to the diffusion limitations of the reactants. A thorough description of the electrochemical characteristics of MFCs demands a detailed investigation of ohmic, kinetic, and mass transport properties. This requires a complete knowledge of the activation and concentration polarization losses at individual electrodes.

Electrochemical impedance spectroscopy (EIS) is a useful tool to investigate these losses and delineate the individual contributions from different resistances to the overall cell impedance (Bard and Faulkner, 2000; Barsoukov and MacDonald, 2005; Orazem and Tribollet, 2006; Park and Yoo, 2003; Scully et al., 1993). Such resistances include ohmic resistances of the cation exchange membrane (if present), electrolyte, and metallic connections, charge transfer and mass transfer polarization resistances on the anode and cathode. With the help of equivalent electrical circuit fitting analysis, EIS can also provide quantitative estimates of the kinetic rate constants for the anodic and cathodic reactions, double layer capacitance at the electrode surface, and the diffusion coefficients of electro-active species in the bulk electrolyte. EIS has been widely used in various areas of electrochemical research such as corrosion (Kelly et al., 2002), batteries (Huet, 1998), and fuel cells (Wagner et al., 1998). Others have used the EIS technique to study MFCs (Cheung et al., 2007; He et al., 2006) but did so with the objective of monitoring the internal resistance under steady-state MFC operation. To our best knowledge, there is no detailed report yet on the influence of microbial growth on the electrochemical impedance or on the kinetics of anodic and cathodic processes. Until now it is unclear whether it is the electrochemical kinetics or electrochemical transport processes that has a direct influence over the power output of an MFC during the initial microbial growth. Also the performance limitations of the anode and cathode and their relative significance in determining the power output in the absence of substrate limitation has not been studied in detail from an electrochemical standpoint. In this article, we report on the variation of electrochemical impedance during initial microbial growth in a two-chamber mixed-culture MFC.

Experimental

MFC Preparation

All experiments were performed in acetate-fed two-chamber MFCs. The set up of the MFCs used in this study was the same as that previously described (Ren et al., 2007). The growth medium in the anode chamber contained (per liter) 1.05 g of NH_4Cl, 1.5 g of KH_2PO_4, 2.9 g of $K_2HPO_4 \cdot 3H_2O$, 0.2 g yeast extract, 10 mL of trace mineral mix, and 10 mL of vitamin mix and had an initial pH of 7.0 (Ren et al., 2007). In addition, 10 mM sodium acetate was used as the electron donor. The cathode chamber was filled with 100 mM of $K_3[Fe(CN)_6]$ solution in 100 mM KH_2PO_4 buffer (pH 7). A 175 μm thick Nafion 117® polymer membrane (sulfonated tetrafluorethylene copolymer) served as the cation exchange membrane separating the two chambers. E-Tek™ microfibrous carbon papers about 350 μm thick and 15 cm^2 geometric area were used as both anode and cathode. A 0.1 M Ag/AgCl reference electrode was installed in the anode chamber for performing electrochemical measurements on individual electrodes. An uncharacterized mixed-culture obtained from anaerobic sludge was inoculated as the biocatalyst in the anode chamber.

MFC Operation

Initial bacterial growth and biofilm development was induced using a 1 kΩ resistive load across the MFC for a few hours until the cell voltage reached a stable value. The growth phase was then allowed to proceed by polarizing the cell to 0.4 V, while simultaneously monitoring the current generated as a function of time. Potentiostatic operation at 0.4 V mimicked the conditions that developed using a 1 kΩ resistive load, while also providing a standard reference point for the comparison of EIS results. The MFC was continuously operated under an external load for 5 days after inoculation, after which it was maintained at open circuit for a week (from days 5 to 12). To provide a reference point for the performance of the initial biofilm development, an identical system was maintained in closed circuit operation for 3 weeks, with three replacements of anode medium and cathode ferricyanide solution during that period.

EIS Experiments

The EIS experiments were performed during the biofilm growth on days 1, 2, 4, and 5 as well as on days 8 and 12 (i.e., when the circuit was open). EIS was also performed on the parallel system after 3 weeks of closed circuit operation. Zahner™ IM6ex potentiostat-AC frequency analyzer equipment was used for the EIS experiments, and the results were analyzed using Thales® software. The frequency of the AC signal was varied from 10 kHz to 100 mHz with an amplitude of ±10 mV. As the maximum operable current for the MFC with immature biofilm was 400 μA, impedance experiments were performed under galvanostatic closed-circuit conditions at 0, 50, 100, 250, and 400 μA for the immature biofilm, and at 0 and 400 μA for the developed biofilm for comparison purposes. To ensure steady state during galvanostatic operation, the MFC was allowed to equilibrate for 10 min between each current setting before applying the AC signal. Impedance measurements were taken on three different configurations designated full cell (FC), anode (A), and cathode (C) as detailed in Table I. The

Table I. Different test cell configurations used for EIS studies.

Configuration	Working electrode (WE)	Reference electrode (RE)	Resistive components in the configuration
Full cell (FC)	Cathode	Anode	Cathode, catholyte, membrane, anolyte, and anode
Anode (A)	Anode	Ag/AgCl	Anode
Cathode (C)	Cathode	Ag/AgCl	Cathode, membrane, catholyte, anolyte

FC configuration measured the impedance contributions from all components of the MFC, while the A and C configurations measured only the impedance of the respective working electrode (WE). Since the reference electrode (RE) was permanently installed in the anode chamber, the cathode impedance taken with respect to the RE also included the membrane and electrolyte resistances. However in the anode configuration, the solution effects were minimized by placing the RE close to the anode. The equivalent electrical circuits shown in Figure 1 was used to fit the impedance data to obtain various electrochemical parameters. The FC Nyquist data were fitted using the electrical circuit given in Figure 1a, with representative parameters for the polarization and ohmic resistances, which does not delineate the individual anode and cathode polarization resistance. For the A and C configurations, this equivalent circuit model consisted of an ohmic resistance component, followed by a Randle's type circuit of an electrochemical charge transfer resistance (R_{ct}) and a Warburg's diffusion element (W) in parallel with a double layer constant phase element (CPE_{DL}) as shown in Figure 1b. The constant phase element is used in the place of a capacitor to simulate the non-ideal behavior of distributed capacitance, typical of porous electrodes (Orazem et al., 2002). W and R_{ct} describe the composite diffusion limitations and charge transfer resistances, respectively, and do not differentiate the contributions from distinct gradients (e.g., electron donor and reduced mediator) or mechanisms of anode reduction (e.g., nanowires and outer membrane cytochromes). While studying the impedance behavior, the MFC must be treated as an electrode-electrolyte system with faradaic and non-faradaic processes. Besides the existence of a complex interaction between the microbiological-biochemical-chemical-electrochemical processes in this system, only those processes that would respond to electrochemical perturbation (i.e., only the electrochemical reaction mechanisms) can be studied by EIS. The measured response would be an intrinsic composite response of all these underlying process, as they would all end up transferring electrons to the electron acceptor. The methodology of equivalent circuit analysis of impedance data is detailed elsewhere (Barsoukov and MacDonald, 2005; Orazem and Tribollet, 2006; Scully et al., 1993).

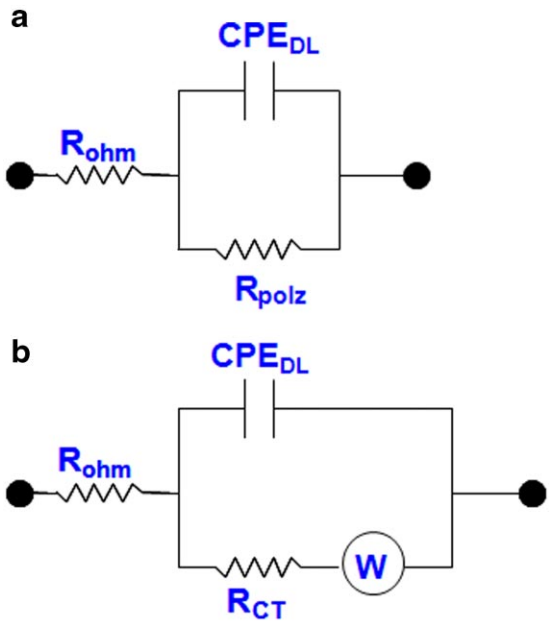

Figure 1. Equivalent circuits used for the analysis of impedance data. **a**: full cell; (**b**) anode and cathode. [Color figure can be seen in the online version of this article, available at www.interscience.wiley.com.]

Experiments were also performed on an abiotic cell using identical substrate and ferricyanide concentrations to evaluate the ohmic resistance of this system in the absence of electrochemical reactions. In this way the membrane and the electrolyte solution resistances were evaluated separately and later subtracted from the impedance measured in the C configuration to separate out the cathode impedance. The impedance results were normalized based on the geometric surface area of the electrodes (15 cm^2), which is much less than the actual electrochemical surface area for porous electrodes. Unlike fuel cell and battery electrodes, the actual functional area of the porous MFC anode cannot be determined using conventional techniques such as BET or porosimetry, which would not account for microbe accessibility or the fact that the bacterial density and anode porosity change during the MFC operation. At a given time, the exchange current density, which is the electrochemical equivalent of a chemical rate constant, can be obtained from the charge transfer resistance (Bard and Faulkner, 2000). For a single or multistep mechanism the charge transfer resistance R_{ct} is defined as follows:

$$R_{ct} = \frac{RT}{nFi_{ex}}$$

where R is the gas constant in J/mol/K, T is the temperature in K, n is the number of electrons involved in the charge transfer reaction ($n = 8$ for acetate oxidation), F is the Faraday's constant in C, and i_{ex} is the exchange current density for the electrochemical reaction.

Results and Discussion

Beginning from day 1 until the onset of day 5, there was continuous biofilm growth as the MFC was kept continuously under load. After day 5, when the cell was open circuited to preclude the use of the anode as an electron acceptor, current was no longer generated by the MFC (except during the EIS experiments). Given the use of a non-fermentable substrate, an inoculum derived from an anaerobic digester, and ferricyanide as the terminal electron acceptor in the cathode, thus avoiding any oxygen diffusion into the anode chamber, the most likely metabolisms between days 5 and 12 were methanogenesis and endogenous decay (Jung and Regan, 2002). Hence it was very likely that the net biofilm growth slowed down or even stopped after day 5. A total of 41 C was extracted from the MFC in 12 days of operation, including the charge extracted during the EIS experiments. Although the residual acetate concentration was not measured, an unreasonably low coulombic efficiency of 1% [compared to 65% reported by Oh et al. (2004) for a wastewater sludge and acetate-fed MFC] would have accounted for the total consumption of only half the added acetate. Such low substrate utilization ensures that our electrochemical measurements were not limited by the electron donor availability. Our previous experience with similar systems, and the shape of the current versus time curve during growth phase, indicates that the growth of the microbial biofilm was incomplete even after a continuous closed-circuit operation for 5 days after inoculation. The parallel system that was operated for 3 weeks showed stable performance, suggesting that the biofilm in this system was essentially established after 3 weeks.

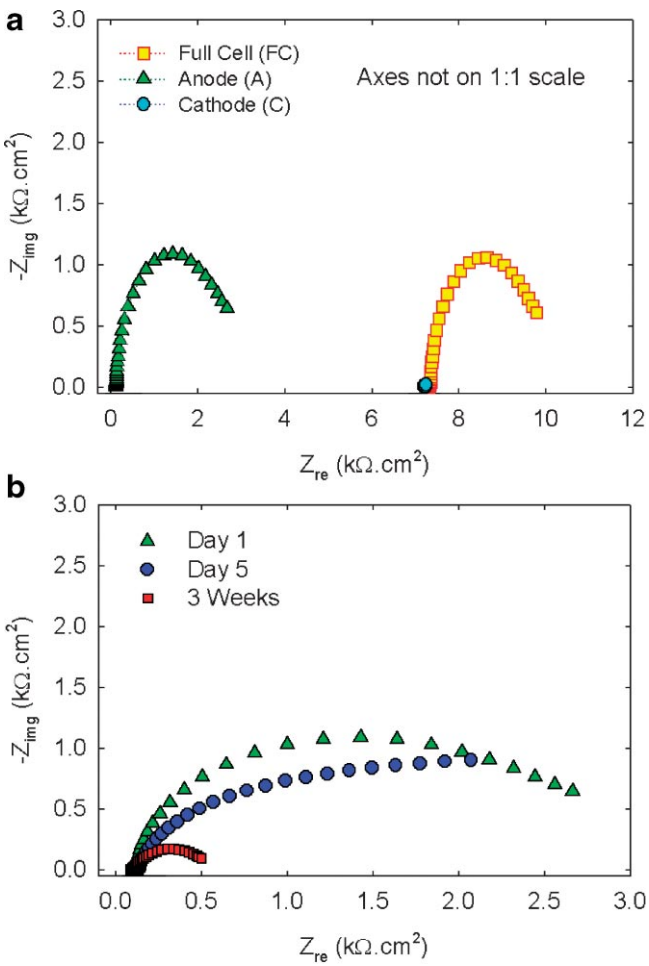

Figure 2. Nyquist plots from a two-chamber MFC obtained at a current of 400 μA (**a**) for the full cell, anode, and cathode configurations after 1 day of operation; and (**b**) for the anode on days 1 and 5 and after 3 weeks for an established biofilm. [Color figure can be seen in the online version of this article, available at www.interscience.wiley.com.]

Impedance of Two-Chamber MFC System

The open circuit voltage of the MFC, measured across the electrodes after inoculation, was between 695 and 700 mV. Nyquist plots for the FC, A, and C configurations at an operating current density of 27 μA/cm^2 (i.e. 400 μA) on day 1 are shown in Figure 2a. The real axis (Z_{re}) intercept of the Nyquist curves in the high frequency region corresponds to the time-independent ohmic resistance in the respective configuration (Barsoukov and MacDonald, 2005; Orazem and Tribollet, 2006; Scully et al., 1993). The ohmic resistances of the FC and C configurations on day 1 were approximately the same (~7.2 kΩ cm^2), while the anode ohmic resistance was comparatively negligible (~0.1 kΩ cm^2). This behavior can be explained from the electrode arrangement in each configuration (Table I). The impedance measured in the C and FC configurations included the membrane and electrolyte resistances, but in the A configuration the RE was placed as close as possible to the anode such that it measured only the anode impedance.

The magnitude of the Nyquist arc qualitatively yields the electrochemical polarization resistance of the working electrode in each configuration, while the quantitative values can be obtained by equivalent circuit fitting of the data (Barsoukov and MacDonald, 2005). The magnitude of the Nyquist curve for both the FC and A configurations are similar in magnitude (Fig. 2a), while that for configuration C is much smaller, indicating that the electrochemical polarization resistance of the MFC was caused almost entirely by the anode for the ferricyanide cathode based systems, even after allowing biofilm development for over 3 weeks (Fig. 2b). This implies that the anode dominated the MFC polarization resistance and limited the kinetics of the bio-electrochemical reaction in this MFC configuration. Using the equivalent circuit shown in Figure 1, the electrochemical polarization resistances of the full cell and anode on day 1 were estimated to be 2.67 and 2.61 kΩ cm^2, respectively, at an operating current density of 27 μA/cm^2, while for the cathode this value was only 0.07 kΩ cm^2. For the MFC with the established biofilm this value was only 0.55 and 0.48 kΩ cm^2 respectively for the full cell and anode, indicating the dominance of anode impedance even in an MFC with established biofilm.

The EIS experiments were also performed at different external loads (currents). Figure 3 shows the Nyquist plots for configuration A at different external currents on day 1. The electrochemical charge transfer resistance (R_{ct}) and double layer capacitance (C_{DL}) of the anode were also estimated by fitting the Nyquist data with the equivalent circuit given in Figure 1b. As expected for any fuel cell system, the electrochemical polarization resistance decreased with increasing current density (Fig. 3). Increasing current densities also require a large driving force especially at the initial stages of biofilm growth and this driving force was available in the form of overpotential on the anode as it moved from −389 mV at open circuit towards more positive values at high currents. However, for the MFC operated for 3 weeks which had the established biofilm, the anode polarization (though dominant over the cathode) was significantly smaller as it only polarized the anode from −486 mV to −440 mV as shown in Figure 4. A comparison of the polarization curves for the full cell and the anode for immature biofilm (5 days) and established biofilm (3 weeks) cases are also shown in Figure 4. Higher over-potentials at high currents led to an enhanced rate of acetate oxidation and hence lowered the R_{ct}. Contrary to other fuel cell systems, an increase in overall impedance was not observed even at very high current densities, indicating that the mass transfer limitations were insignificant and masked by the dominant kinetic limitations for the anode bio-electrochemical reaction. The expected shape of Nyquist plots for diffusion-limited electrochemical systems would have a 45° curve extending to very low frequencies (Ramasamy et al., 2006), which was not observed in this study.

Effect of Microbial Growth on Anode Kinetics and Power Output

The kinetic impedance, R_{ct}, of the anode at different stages of the microbial growth was evaluated from the EIS data

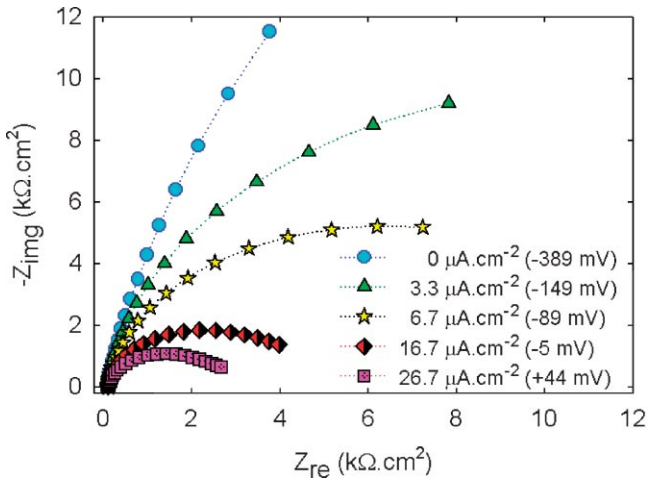

Figure 3. Nyquist plots for the anode configuration at different external current densities on day 1. The anode potentials shown in the legends are obtained with respect to Ag/AgCl. [Color figure can be seen in the online version of this article, available at www.interscience.wiley.com.]

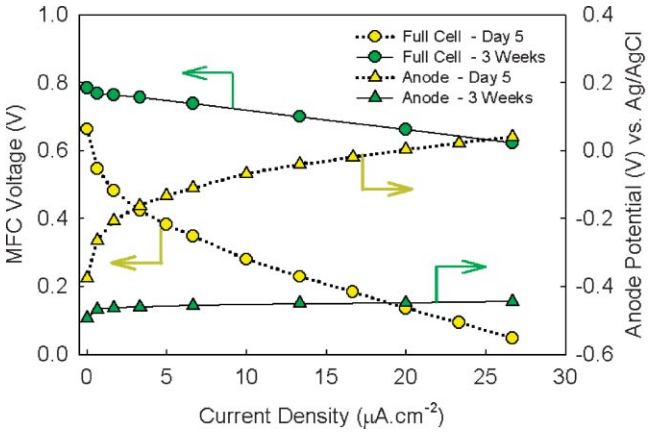

Figure 4. Comparison of full cell and anode polarization curves after 5 days (immature biofilm) and after 3 weeks (developed biofilm). [Color figure can be seen in the online version of this article, available at www.interscience.wiley.com.]

obtained on different days (Fig. 5). There was a rapid decrease in the R_{ct} during the first 5 days by over 40% from 2.6 to 1.5 kΩ cm^2, during which period the microbial growth was continuously induced by the external load. This indicates that the microbial growth on the anode has a beneficial effect on the kinetics of the bio-electrochemical reaction as it decreases the anode activation losses due to increased biocatalyst density. After day 5, the MFC was open circuited, hindering the biochemical reactions due to the absence of an electron acceptor. As a result, the anode biofilm growth slows down after day 5, which is suggested by the change in the slope of the curve in Figure 5. However between days 8 and 12, the trend reversed and R_{ct} showed a slight increase. This may be due to an increasingly inactive biofilm for electrochemical reactions although there is no conclusive evidence to confirm this using our current experiments. The parallel system that was operated in closed

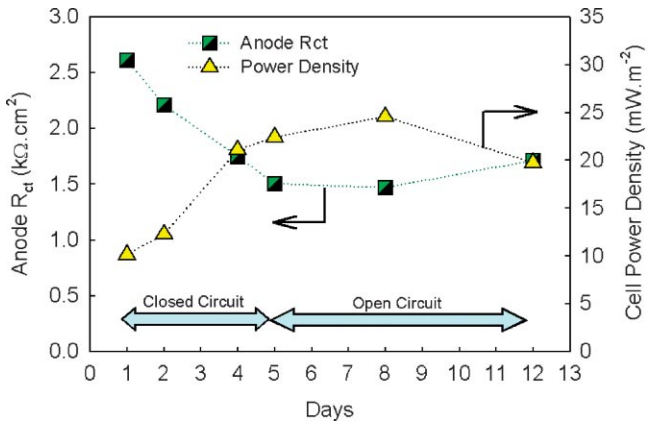

Figure 5. Variation of the anode R_{ct} and the MFC power density with time at a current density of 27 μA/cm^2. [Color figure can be seen in the online version of this article, available at www.interscience.wiley.com.]

circuit for 3 weeks had an R_{ct} of 0.48 kΩ cm^2, a 60% reduction from the first 5-day performance. The typical values for double layer capacitance in our results varied from 0.5 to 0.9 mF for a 15 cm^2 anode, which agrees well with the expected capacitance of a carbon electrode (Bard and Faulkner, 2000; Orazem and Tribollet, 2006).

Figure 5 also shows the variation of MFC power density as a function of time. The power density shown in the figure was obtained at 400 μA (i.e. 27 μA/cm^2) and does not represent the peak power delivered by this MFC. The MFC power density increased along with the microbial growth until day 8, after which it began to decrease. Although not shown on Figure 5, the power density after 3 weeks of operation in the parallel system was 166 mW/m^2, and the maximum operable current density for this MFC with the established biofilm was 0.1 mA/cm^2 which was 5–6 times higher than that reported in the literature for other two chamber designs (Bond and Lovley, 2003; Liang et al., 2007). It is unclear why the power density increased slightly between days 8 and 5, given that the system was operated with an open circuit during this period. The power density curve followed the reciprocal trend as that of the R_{ct} curve, although not linearly proportional to one another. This was expected, as the current output from the MFC increased steadily during the microbial growth phase. However it is important to ensure that the variation in power density at 27 μA/cm^2 was not caused by the variation in the cathode potential. The continuous reduction of ferricyanide to ferrocyanide at the cathode causes the cathode potential to vary over time during the MFC operation. While the open circuit potential of the cathode voltage (vs. Ag/AgCl) varied as much 25 mV during the 12 days of operation, at 27 μA/cm^2 this variation was only 7 mV, which was insufficient to increase the MFC power density by 14 mW/cm^2 between days 1 and 8. Thus it was presumed from these results that higher bacterial density in the biofilm helped achieve higher power output by enhancing the electrochemical reaction rate, which resulted in higher currents for the same operating voltage. Picioreanu et al. (2007) suggested from their modeling results that an excessively thick biofilm could negatively influence the power density by increasing the biofilm electronic resistance or by causing substrate diffusion limitations inside the pores of the anode. This outcome was not observed during our initial biofilm growth study, but might emerge under longer-term operation of these systems.

Figure 6 shows the variation of R_{ct} with current external currents (loads) before the biofilm formation (day 1), after significant biofilm growth (day 5), and during biofilm stagnation or decay (day 12). It is interesting to note that the anode R_{ct} after 5 days of continuous microbial growth was significantly lower than that of the initial R_{ct} (day 1) for all operating current densities. Also, the R_{ct} varied only slightly upon leaving the MFC at open circuit for about a week after day 5. The R_{ct} is an indirect measure of the kinetics of the electrochemical reaction. The rate of electrochemical reaction is often expressed as the exchange current density

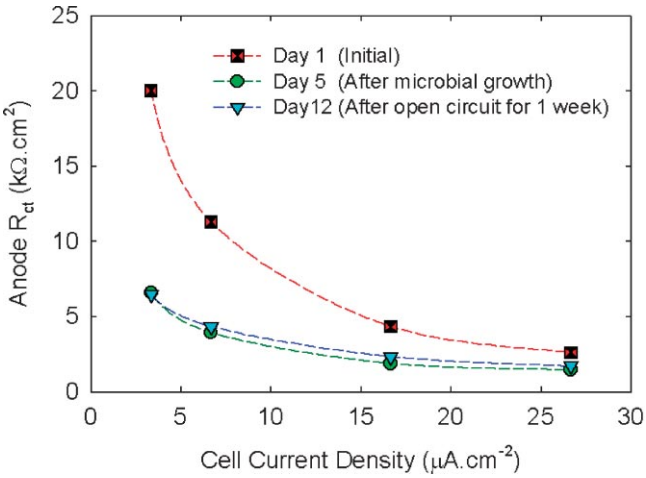

Figure 6. Variation of anode R_{ct} with current density for different days obtained by equivalent circuit fitting of the corresponding Nyquist data. [Color figure can be seen in the online version of this article, available at www.interscience.wiley.com.]

(i_{ex}), which is an important kinetic parameter for electrochemical modeling. The i_{ex} calculated from the R_{ct} at open circuit varied from 40 nA/cm^2 (day 1) to 58 nA/cm^2 (day 5), and was 182 nA/cm^2 in the parallel system after 3 weeks of closed-circuit operation.

Performance Limitations of Two-Chamber Design

The power densities of two-chamber MFC designs are known to be constrained because of their high internal resistance. However, little work has been done so far to quantify the various components of the MFC internal impedance such as solution ohmic resistance, anode and cathode kinetic impedance, and mass transfer impedance. The dominant contribution of the membrane and solution to the ohmic resistance in a two-chamber design was confirmed through two separate EIS measurements performed on abiotic cells with identical substrate and ferricyanide concentrations as described in the experimental section. In the first case, the cathode impedance was evaluated with respect to an RE installed adjacent to the cathode. Results from this experiment showed that the ohmic resistance of the cathode was less than 2% of the overall ohmic resistance of the cell. In the second experiment, the combined membrane and solution ohmic resistance was evaluated with an identical two-chamber cell in the absence of microbes, such that there were no bioelectrochemical reactions. In this case, the combined membrane and solution ohmic resistance was typically about 90–95% of the full cell ohmic resistance at open circuit. The results from these two experiments confirmed that the ohmic component of MFC internal impedance was dominated by the solution and membrane in a two-chamber design. However, the membrane or solution does not

have an influence over the electrochemical polarization resistance under load conditions. The domination of ohmic resistance in a two chamber system has also been confirmed by others (Liang et al., 2007) who studied the composition and distribution of internal resistance in three MFC designs.

Figure 7a shows the ohmic resistances of A, C, and FC configurations at different operating densities after microbial growth. Using the ohmic resistances of membrane and solution determined in the abiotic test, this value was then subtracted from the ohmic resistance measured using C configuration to obtain the cathode ohmic resistance without the membrane and solution effects. As per theory, the ohmic resistances in Figure 7a did not vary with current density. Note that the values in Figure 7a are only the ohmic part of the MFC total impedance and do not include the electrochemical polarization resistance (kinetic or mass transfer effects). In other words, the values represent the intercept of the Nyquist arc on the *x*-axis and do not include the magnitude of the arcs themselves. The ohmic contribution of the anode and cathode to the overall MFC ohmic resistance was less than 3% while the membrane, electrolyte, and cathode together contribute over 95% of the MFC ohmic resistance in the two-chamber design used for this study. The values in Figure 7a do not always add up to 100% because of some ambiguity in the equivalent circuit fitting interpretation (Park and Yoo, 2003). The kinetic and mass transfer resistances are masked by the high ohmic resistance of these two-chamber systems, but would be more pronounced in recent single-chamber MFC designs with reduced ohmic resistance (Liu and Logan, 2004).

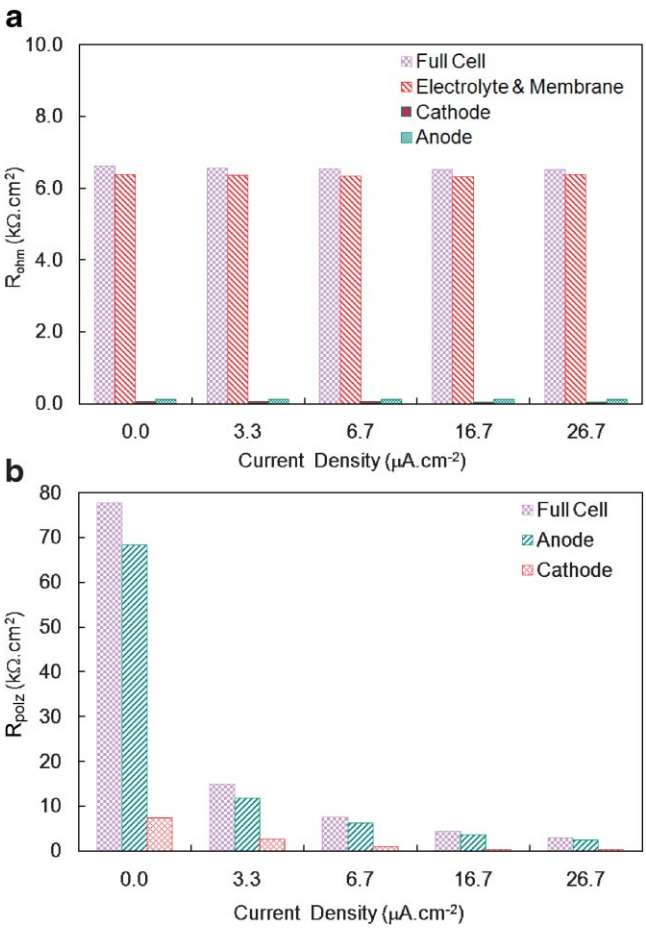

Figure 7. **a**: Ohmic resistance measured in FC, C and A configurations on day 8. **b**: Electrochemical polarization resistances of full cell, cathode and anode on day 8. The polarization resistance includes both kinetic and mass transfer resistances. [Color figure can be seen in the online version of this article, available at www.interscience.wiley.com.]

The electrochemical polarization resistances of anode, cathode and full cell after microbial growth for 8 days are compared in Figure 7b. The values were obtained by fitting the Nyquist data with an equivalent circuit similar to the one shown in Figure 1b, which combines the kinetic (R_{ct}) and mass transfer (W) resistance into a single parameter, the electrochemical polarization resistance R_{polz}. The electrochemical polarization resistances do not arise from membrane or electrolyte solution. It is clear from Figure 7b that the anode dominates the electrochemical polarization resistance of this MFC, in a ferricyanide catholyte system. However if the cathode involves the oxygen reduction reaction, which is a kinetically sluggish reaction, a variation in this balance could occur as observed in our experiments (Ramasamy et al., 2007a,b). Although not explicit from Figure 7b, the ratio of kinetic to mass transfer resistances of the anode decreases with current density. This is due to the over potential effect. At larger over potentials (high currents), the electrochemical reactions are more facile and not limited by the kinetics. Instead the reactions are limited by the availability of the reactants at the electrochemical interface. This would mean an increased mass transfer resistance at high current and hence the above mentioned ratio decreases with increasing current density.

Conclusions

For the first time, the different intrinsic resistances of the MFC have been quantified and correlated with the initial biofilm growth. The kinetic rate constant or the exchange current density for the anode bio-electrochemical oxidation was estimated to be in the range of 40 to 60 nA/cm^2 during initial biofilm development, and increased to 182 nA/cm^2 for an established biofilm. The values of R_{ct} and i_{ex} indicate that the rate of the bio-electrochemical reaction in these two-chamber MFCs was over four orders of magnitude lower than that of typical hydrogen fuel cell reactions. The growth of the microbial biofilm was found to decrease the anode polarization resistance and facilitate the kinetics of the electrochemical reactions. Also the slow biofilm degradation or alternate metabolisms in the absence of the anode as an electron acceptor were found to decrease the catalytic activity, indicated by the slow increase in R_{ct} of the anode. For the ferricyanide-based MFC system studied here, the cathode polarization resistance was insignificant

when compared to that of the anode, even for a fully developed biofilm. Our results clearly indicate that apart from the dominant ohmic resistance arising from the membrane and electrolyte solution, the anode suffers from severe kinetic limitations reflected as a high R_{ct}, especially at low to medium current densities. Improvements in MFC architectural design have focused on minimizing the ohmic component of the overall internal MFC impedance. In such improved architectural designs, the anode kinetic limitations as inferred from our EIS experiments would play a more important role in determining the overall power output of MFCs.

References

Bard AJ, Faulkner LR. 2000. Electrochemical methods: Fundamentals and applications, 2nd edition. New York: John Wiley & Sons.

Barsoukov E, MacDonald JR. 2005. Impedance spectroscopy: Theory, experiment and applications, 2nd edition. New York: Wiley InterScience.

Bond DR, Lovley DR. 2003. Electricity production by *Geobacter sulfurreducens* attached to electrodes. Appl Environ Microbiol 69(3):1548–1555.

Cheng S, Liu H, Logan BE. 2006. Increased power generation in a continuous flow MFC with advective flow through the porous anode and reduced electrode spacing. Environ Sci Technol 40:2426–2432.

Cheung ACM, Bretschger O, Mansfeld F, Nealson KH. 2007. Performance of different strains of the sensus Shewanella in a microbial fuel cell. Abstract # 127, 234th ACS National Meeting, Aug 19–23, Boston.

He Z, Wagner N, Minteer S, Angenent L. 2006. An upflow microbial fuel cell with an interior cathode—Assessment of the internal resistance by impedance spectroscopy. Environ Sci Technol 40(17):5212–5217.

Huet H. 1998. A review of impedance measurements for determination of the state-of-charge or state-of-health of secondary batteries. J Power Sources 70:59–69.

Jung S, Regan JM. 2002. Comparison of anode bacterial communities and performance in microbial fuel cells with different electron donors. Appl Microbiol Biotechnol 77:393–402.

Kelly RG, Sculy JR, Shoesmith D, Buchheit RG. 2002. Electrochemical techniques in corrosion science and engineering, 1st edition. New York: CRC.

Liang P, Huang X, Fan MZ, Cao XX, Wang C. 2007. Composition and distribution of internal resistance in three types of microbial fuel cells. Appl Microbiol Biotechnol 77:551–558.

Liu H, Logan BE. 2004. Electricity generation using an air cathode single chamber microbial fuel cell in the presence and absence of proton exchange membrane. Environ Sci Technol 38:4040–4046.

Logan BE, Regan JM. 2006a. Electricity producing bacterial communities in microbial fuel cells. Trends Microbiol 14(12):512–518.

Logan BE, Regan JM. 2006b. Microbial fuel cells: Challenges and applications. Environ Sci Technol 40(17):5172–5180.

Min B, Cheng S, Logan BE. 2005a. Electricity generation from cysteine in a microbial fuel cell. Water Res 39(5):942–952.

Min B, Cheng S, Logan BE. 2005b. Electricity generation using membrane and salt bridge microbial fuel cells. Water Res 39(9):1675–1686.

Oh SE, Min B, Logan BE. 2004. Cathode performance as a factor in electricity generation in microbial fuel cells. Environ Sci Technol 38(18):4900–4904.

Orazem ME, Tribollet B. 2006. Electrochemical impedance spectroscopy. New York: Wiley InterScience.

Orazem ME, Shukla P, Membrino MA. 2002. Extension of the measurement model approach for deconvolution of underlying distributions for impedance measurements. Electrochim Acta 47(13):2027–2034.

Park SM, Yoo JS. 2003. Electrochemical impedance spectroscopy for better electrochemical measurements. Anal Chem 75:455A–461A.

Picioreanu C, Head IM, Katuri KP, Van Loosdrecht MCM, Scott K. 2007. A computational model for biofilm based microbial fuel cell. Water Res 41(13):2921–2940.

Ramasamy RP, Feger C, Strange T, Popov BN. 2006. Discharge characteristics of silver vanadium oxide cathodes. J App Electrochem 36(4):487–497.

Ramasamy RP, Ren Z, Mench MM, Regan JM. 2007a. Microbial fuel cells for waste water treatment. ECS Transactions, 212th Meeting of the Electrochemical Society, October 7–12, Washington D.C.

Ramasamy RP, Ren Z, Mench MM, Regan JM. 2007b. Electrochemical impedance spectroscopy studies on microbial fuel cells. 234th ACS National Meeting Fuel Chemistry Division Preprints 52(2): 539.

Ren Z, Ward TE, Regan JM. 2007. Electricity production from cellulose in a microbial fuel cell using defined binary culture. Environ Sci Technol 41(13):4781–4786.

Scully JR, Silverman DC, Kendig MW. 1993. Electrochemical impedance: Analysis and interpretation. Philadelphia, PA: ASTM International.

Wagner N, Schnurnberger W, Muller B, Lang M. 1998. Electrochemical impedance spectra of solid-oxide fuel cells and polymer membrane fuel cells. Electrochim Acta 43(24):3785–3793.